Simulation numérique 3D du foudroyage d'une exploitation par panneaux à grande échelle

Samar Ahmed, Marwan Al Heib, Yann Gunzburger, Vincent Renaud

SIMULATION NUMERIQUE 3D DU FOUDROYAGE D'UNE EXPLOITATION PAR PANNEAUX A GRANDE ECHELLE

3D NUMERICAL SIMULATION OF THE GOAF DUE TO LARGE SCALE LONG-WALL MINING

Samar AHMED[1], Marwan ALHEIB[2], Yann GUNZBURGER[1], Vincent RENAUD[2]
[1] *GeoRessources, CNRS, Ecole des Mines, Nancy, France*
[2] *INERIS, Ecole des Mines, Nancy*

RÉSUMÉ – La simulation du foudroyage d'une exploitation par longues tailles est essentiel pour d'exploitation à large échelle. Afin d'évaluer les variations des champs de contraintes et de déplacement dans une mine de Provence, le foudroyage est simulé par modélisation numérique en prenant en compte sa géométrie et ses propriétés mécaniques équivalentes. L'évolution spéciale et temporelle des caractéristiques des matériaux foudroyés est simulée en appliquant une variation linéaire du module de Young, calée par rapport à la aux mesures d'affaissement en surface.

ABSTRACT – The simulation of the goaf area associated with panels is essential in large scale mines. In this study, the goaf area is simulated by using elastic numerical modelling, to assess the stress and displacement field changes in a Provence coalmine with taking into account the goaf geometry and its equivalent mechanical properties. The evolution in space and in time Heterogeneity of the goaf material is simulated by using linearly varying elastic modulus, which has been calibrated with the surface subsidence measurements.

1. Introduction

Longwall mining method is widely used especially in coal mines which involves removal of large rectangular panels. As the coal panel is exploited, the roof and floor of the excavation becomes in contact and the rockmass is caved. (Peng and Chiang, 1984) considered that after the disturbance of long-wall caving excavation, the above volume will divide into three different zones as shown in Fig. (1).

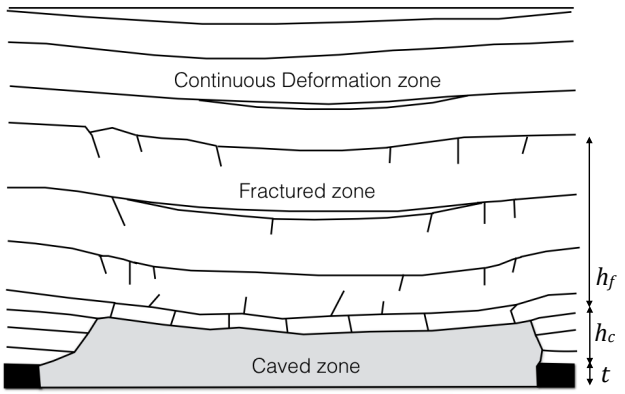

Figure 1. Three zones of disturbance due to long-wall caving mining method.

The caved zone is the much fragmented zone where the roof totally collapses into the floor of the excavation. (Kenny, 1969) performed in-situ measurements in order to determine the height of the caved zone. He found that for a seam with height (t), the caved zone height

(h_c) is equal to (2 – 4) *t*. While (Hasenfus et al., 1998) found that h_c is equal to (4 – 6) *t*, recently (Shabanimashcool, 2012) proposed that $h_c = 4t$ based on the numerical modeling results. The second influenced zone is the fractured zone which lies directly above the caved zoned, where the strata are broken into blocks associated with major horizontal and vertical crakes and bed separation. (Peng and Chiang, 1984) proposed that the fractured zone height (h_f) is equal to (28 – 42) times the seam thickness (*t*). The last zone is the continuous deformation zone, where the rock mass behaves as a continuous medium.

The principal issue in the goaf area (caved zone + fractured zone) numerical simulation is the assessment of the mechanical behavior of the goaf material which is very difficult due to the inaccessibility to the damaged area as well as the heterogeneity of the material itself. Many researches have been released to assess numerically the mechanical properties of the goaf area. (Kose and Cebi, 2010) suggested a wide interval of elastic module within the goaf area as (15 - 3500) MPa. While (Tajdus, 2009) applied a back analysis method for determining the values of rock mass parameters for areas disturbed by mining influence in eleven areas of polish mine. Tajdus found that the elastic moduli in horizontal direction and in vertical direction are very low, in range of (50 – 150) MPa. (Cheng et al., 2010) and (Jiang et al., 2012) assigned goaf material with elastic modulus and Poisson ratio 190 MPa and 0.25 respectively. (Salamon, 1990) defined the stress strain relationship of the goaf material as:

$$\sigma = \frac{E_0 \varepsilon}{1 - (\varepsilon/\varepsilon_m)} \tag{1}$$

where, ε and σ are the vertical strain and stress respectively and E_0 is the initial elastic modulus of the goaf material. ε_m is given by Eq. (2) using the buckling factor BF:

$$\varepsilon_m = \frac{BF - 1}{BF} \tag{2}$$

E_0 (MPa) can be calculated as a function of the unconfined compressive strength of the intact rock, σ_c, and the buckling factor, (Pappas and Mark, 1993) and (Yavuz, 2004):

$$E_0 = \frac{10.39\ {\sigma_c}^{1.042}}{BF^{7.7}} \tag{3}$$

Salamon's model is valid for cave-in materials under hardening condition, (non-elastic) behavior. E_0 and ε_m must be detected firstly then the hardening table will be estimated by using Eq. (1).

(Wilson, 1980) suggested that, after consolidation of the goaf, the vertical stress within the goaf increases linearly from zero at the ribside to the pre-mining vertical stress at a distance from the ribside equal to (0.3 – 0.4) times *H* where *H* is the mining depth. (Wilson, 1982) also suggested that the peak vertical stress on the ribside (the "abutment pressure") might be as high as six time the initial one. The generally accepted stress re-distribution developed by (Wilson, 1982) is as shown in Fig. 2. However, Wilson proposed a 2D estimation and he did not consider the effect of the third direction that may be play an important role. Also, he did not refer to the material properties and its effect in stress redistribution.

The aim of this research is to simulate numerically, by using the elastic model, the goaf area above the excavated panel as well as to assess mechanically the long-wall mining consequence. The goaf area will be presented as an elastic material with a certain geometry and with an elastic modulus various linearly with the height. The geometry and the mechanical properties of the goaf area will be calibrated with the convergence between the roof and the floor as well as the in-situ measurements of the subsidence at the surface.

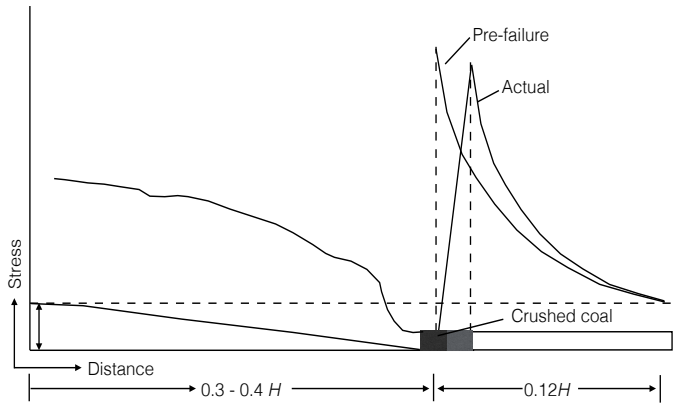

Figure 2. Vertical stress distribution within the goaf and the ribside (Wilson, 1982).

2. Case study

The current case study is the Provence coalmine, located in the south of France. It had been exploited between 1984 and 2004 using the long-wall mining method, with a panel width of 200 m with various lengths. The average thickness of the exploited coal seam is t=2.5 m, at a depth of 700 to 1250 m. The overburden is mainly composed of Fuvelian limestone and Begudo-Rognacian limestone and marl as shown in Fig. 3. The stiffness of the Rognacian layer is low compared with the adjacent Fuvelian layer because it contains a high percentage of marl and clayey limestone, (Gaviglio, 1985). The initial mechanical properties of the different layer within the rockmass are given in Table 1, (Gaviglio et al., 1996). The estimation of the mechanical properties takes into account the rock mass quality and the characterization from laboratory tests.

Table 1: Rock mass mechanical properties.

Rock type	***E* (GPa)**	ν	ρ **(kg/m^3)**
Rognacian	1	0.25	2400
Fuvelian	8.4	0.24	2400
Lignite coal	3	0.32	1500
Jurassic	17	0.25	2400

3. Numerical model

A 3D numerical model of the mine was constructed using the finite difference code FLAC^{3D} (Fig. 3). Four different rock types are specified: the coal seam, the Fuvelian, Rognacian with height 400 m and 600 m above the coal seam, respectively, and Jurassic limestone beds below.

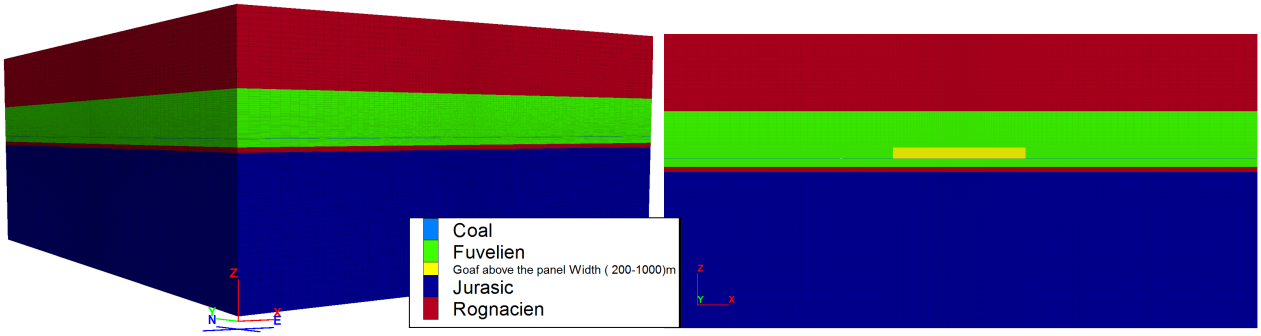

Figure 3. 3D and 2D view of the model showing the mining panel and the goaf area.

The overall dimensions of the model are 4600 m in the x- direction, 6020 m in the y-direction and 2270 m in the vertical direction (z). The top of the model coincides with the ground surface at level z = 0.0 while the excavated panels lies at depth of 1000 m below the surface. This model contains 2.5 million mesh with a very high precision near to the excavated zone in order to overcome the mesh effect. The mechanical properties in Table 1 were used as input data in the numerical model.

4. Goaf simulation Methodology

In the current study, the goaf simulation is composed of two different steps. The first step is to estimate the geometry of the goaf (caved zone and fractured zone), the height of the goaf is taken as 32*t* where *t* (coal seam thickness) = 2.5 m (i.e. $h_{\text{caved-zone}}$=4*t,* (Shabanimashcool et al., 2012) and $h_{\text{fractured-zone}}$=28*t* according to (Peng and Chaing, 1984). The second step, which the current study concerns, is to estimate numerically the mechanical properties within the goaf area. The elastic modulus within the goaf will be calibrated with the convergence between the roof and the floor for 200 m panel width and with subsidence at the surface until 1400 m excavation width that corresponds to the critical width (Al Heib, 1993).

In this model, the elastic modulus (*E*) of the goaf area is assumed to vary linearly with the goaf height (32*t*) as shown in Fig. (4). The elastic modulus begins from a certain value $E_{immediate\text{-}roof}$ directly above the opening and increases linearly within the goaf until $E_{hostrock}$ at 32*t* where is the end of the goaf geometry as defined before. Eq. (4) was fitted to estimate E_{goaf} at any point within the goaf, by assuming that the Poisson ratio is $\upsilon_{goaf} = \upsilon_{hostrock}$ and the direct roof above the excavation has $E_{immediate\text{-}roof}$. The only value that could be changed in this model is the $E_{immediate\text{-}roof}$.

$$E_{goaf(hg.t)} = \left(\frac{E_{hostrock} - E_{immediate-roof}}{x.t} . h_g . t\right) + E_{immediateroof} \quad \text{(MPa)} \qquad (4)$$

Where (x.*t* = 32*2.5 = 80 m) is the maximum height of the goaf that corresponds $E_{goaf(32.t)}$, (h_g.*t*) is the height corresponds to $E_{goaf(hg.t)}$, h_g ranges between (1 – 32) and *t* is the coal seam thickness.

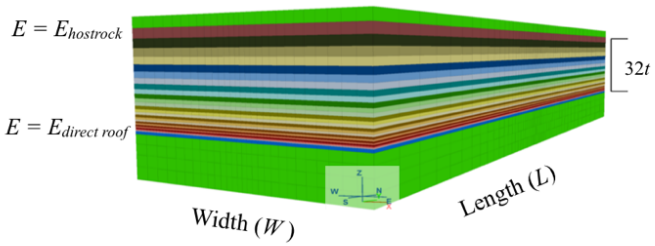

Figure 4. Linear variation of elastic modulus within the goaf area.

In order to satisfy the convergence between the roof and the floor of the excavation (i.e. *convergence = mining seam thickness (t)*), we found that the $E_{immediate\text{-}roof}$ must have 180 MPa maximum as shown in Fig. (5).

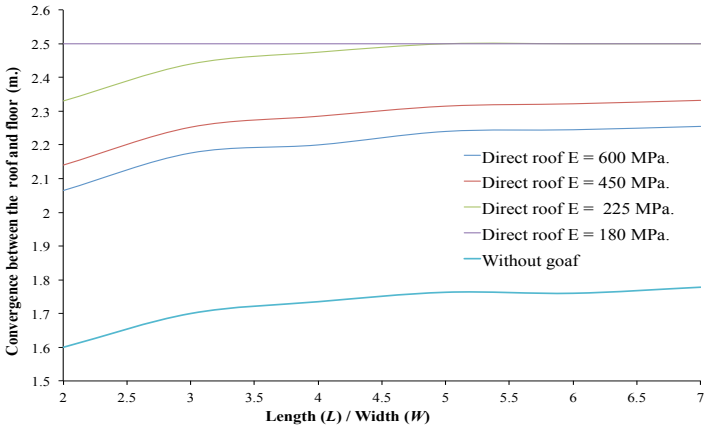

Figure 5: Total convergence between the roof and floor for different panel lengths.

For that, Eq. (4) will be modified to be as follow:

$$E_{goaf(hg.t)} = \left(\frac{E_{hostrock} - 180}{80} . h_g . t\right) + 180 \quad \text{(MPa)} \tag{5}$$

The excavation progress will be performed at once; the consequence of excavation is as shown in Fig. (6). After excavation of each panel the elastic modulus of the goaf area above it will be modified to obey Eq. (5). Fig. (6) shows the variation of the elastic modulus within the goaf area from step 1 (excavation of panel 200 m width) until step 7 (excavation of panel 1400 m width). As shown in Fig. (6) the minimum elastic modulus is directly above the excavated area. In order to calibrate the geometry and the mechanical properties of the goaf area, a general flowsheet of the modelling process has been followed as shown in Fig. (7).

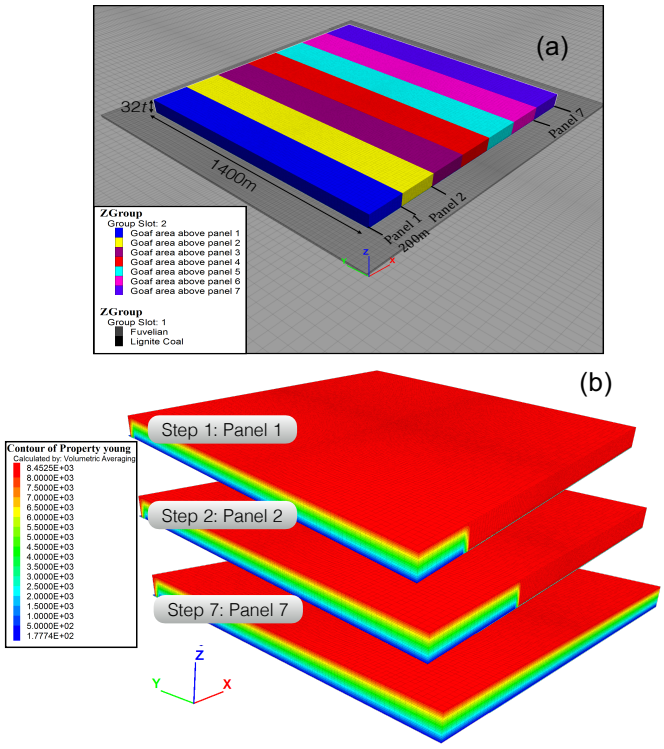

Figure 6. Excavation sequence of the coal panels and elastic modulus variation within the goaf area.

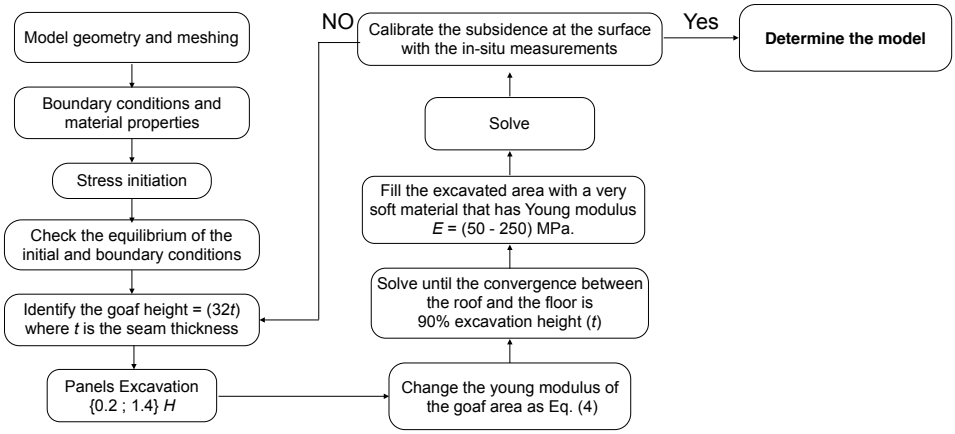

Figure 7. General flowsheet of modelling process.

5. Results and discussion

In order to obtain the applicability of the proposed methodology, the maximum surface subsidence has been recorded at the surface of the model which is assumed to be the surface of the earth in case of Provence coal mine case study. The first calculation has considered that the goaf geometry extends 32*t* above the excavated panel for all the panel widths (200 – 1400 m). Fig. (8a) shows the surface subsidence obtained by the numerical model compared with the in-situ measured values.

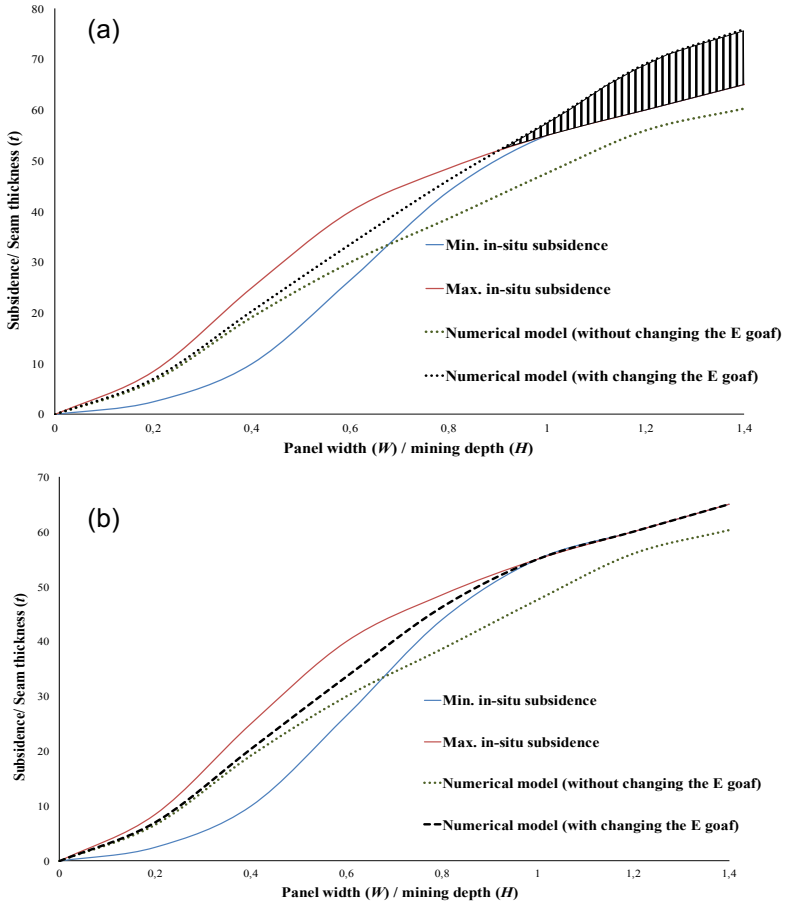

Figure 8. Numerical and in-situ measurement of the subsidence-seam thickness ratio for various panel width-mining depth ratio (a) goaf height 32*t* (b) goaf height vary with the panel width.

It is clearly shown that changing the elastic modulus within the goaf area has an influence on the surface compared the other model. However, the proposed model with 32*t* height of goaf gave overestimated values of surface subsidence for the excavation with width larger than the mining depth.

For that, according the consolidation over the time, we suggested decreasing the goaf height (32*t*) for the panel width larger than 1000 m as shown in Fig. (8b) in order to decrease the surface subsidence to be calibrated with the in-situ measurements. To fit the in-situ surface subsidence measurements in case of panels with different widths 1*H*, 1.2*H* and 1.4*H*, the the goaf height should be :30*t*, 28*t* and 26*t*, respectively. The *x* factor in Eq. (6) could be classified according to the panel with to mining width ratio as follows:

$$E_{goaf(hg.t)} = \left(\frac{E_{hostrock} - 180}{x.t} \cdot h_g.t\right) + 180 \quad (6)$$

i) $W/H = 0.2 – 0.8$, $x = 32$ ii) $W/H = 1.0$, $x = 30$
iii) $W/H = 1.2$, $x = 28$ iv) $W/H = 1.4$, $x = 26$

We can note that the height of the goaf decreases with increasing of the mining width, or in another word the influenced zone due to an excavation become smaller with mining advance which could be the effect of the consolidation of the fragmented rock.

The next step after obtaining the goaf geometry and mechanical properties is comparing the induced vertical stresses to the initial values. Fig. (9) illustrates the normalized vertical stress (induced vertical stress/initial vertical stress) for different panel width to depth ratios. We can notice that the induced vertical stress will be equal to the initial value at (*0.6 – 0.7H*) which is compatible with the values obtained by (Wilson, 1982). As shown in Fig. 2. (Wilson, 1982b) proposed that the induced vertical stress equals the initial values at (0.3 *H* – 0.4 *H*), however, he did not provide any effect of the third dimension (the panel length).

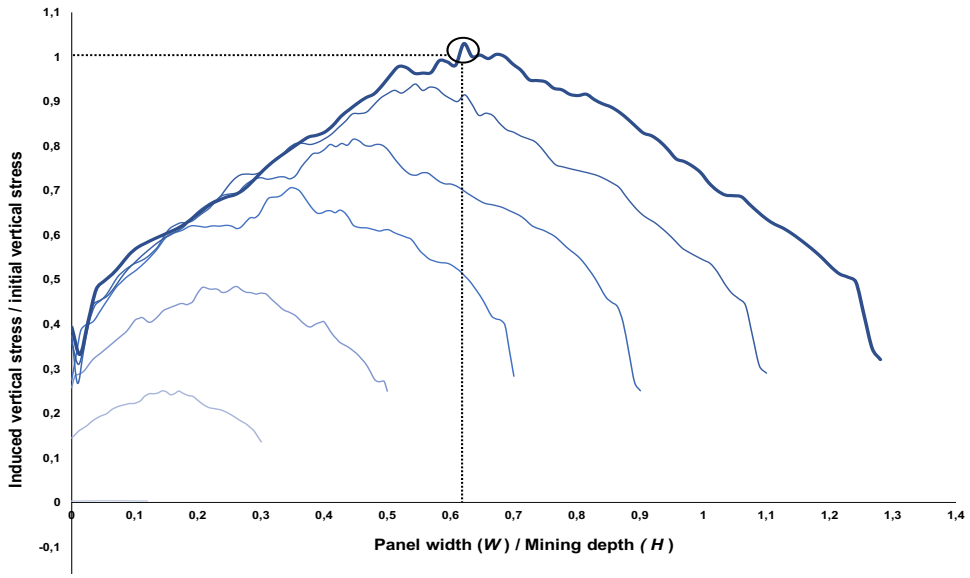

Figure 19. Ratio between induced vertical stress and initial vertical stress

6. Conclusion

This research concerns the simulation of the goaf area associated with long-wall caving panels of the Provence coal mine. We proposed a methodology for the modeling process in order to be able to calibrate the model with the convergence between the roof and the floor of the panel as well as the in-situ measurements of the surface subsidence. We assumed that the height of the goaf zone initially is 32*t*, where *t* is the coal seam thickness. In addition,

the elastic modulus varies linearly within the goaf zone from $E_{immediate\text{-}roof}$ for the direct roof above the excavation, until $E_{host\text{-}rock}$ where the excavation effect will disappear. Based on many iterations have been performed, we found that the $E_{immediate\text{-}roof}$ is 180 MPa at maximum to satisfy the total convergence between roof and floor of the excavation.

The methodology was applied on several panel width (W) to mining depth (H) ratios. The goaf height varied linearly within this height is sufficient to reproduce rational values of surface subsidence for W/H less than 1. However, this proposition gave over estimation of the surface subsidence in case of $W/H \geq 1$. For that, the goaf height was reduced in order to calibrate the model with the in-situ measurements. We noticed that the goaf height decreases with face advance, which could be the effect of the consolidation of the fragmented rocks.

Reference

Peng S.S., Chaing H.S. (1984). Longwall Mining. John Wiley & Sons Inc., New York, pp. 17–73.

Kenny P. (1969). The caving of the waste on longwall faces. Int. J. Rock Mech. Mining Sci. Abstr, vol. 6, pp. 541–555.

Hasenfus G.J., Johnson K.L., Su D.W.H. (1998). A hydrogeomechanical study of overburden aquifer response to longwall mining. In: Peng Syd, S. (Ed.), Proceedings of the 7th International Conference on Ground Control in Mining. Morgantown, West Virginia University, COMER, Department of Mining Engineering, pp. 149–162.

Shabanimashcool M., Charlie C.L. (2012). Numerical modelling of longwall mining and stability analysis of the gates in a coal mine. Int. J. Rock Mech. Mining Sci, vol. (51), pp. 24–34.

Kose H., Cebi Y. (1988). Investigation the stresses forming during production of the thick coal seam. 6th coal congress of Turkey, Zonguldak, pp. 371-383.

Tajdus K. (2009). New method for determining the elastic parameters of rock mass layers in the region of underground mining influence. Int. J. Rock Mech. Mining Sci, vol. (46), pp.1296 – 1305.

Cheng Y.M., Wang J.A., Xie G.X., Wie W.B. (2010). Three-dimensional analysis of coal barrier pillars in tailgate area adjacent to the fully mechanized top caving mining face. Int. J. Rock Mech. Mining Sci, vol. (47), pp. 1372 – 1383.

Jiang Y., Wang H., Xue S., Zhao Y., Zhu J., Pang X. (2012). Assessment of mitigation of coal bump risk during extraction of an island longwall panel. Int. J. Coal Geol, vol. (95), pp. 20 – 33.

Salamon M.D.G. (1990). Mechanism of caving in longwall mining. Proceedings of the 31st US rock mechanical symposium, Golden, Colorado. Rotterdam: Balkema, pp. 161–68.

Wilson A. H. (1982). Pillar stability in longwall mining. State of the Art of Ground Control in Longwall Mining and Mining Science, SME, New York; pp. 85-95.

Wilson A.H. (1980). The stability of underground workings in the soft rocks of coal measures. Unpublished Ph.D Thesis, Univ. Nottingham.

Yavuz H. (2004) An estimation method for cover pressure re-establishment distance and pressure distribution in the goaf of longwall coal mines. Int. J. Rock Mech. Mining Sci, vol. (41), pp. 193–205.

Gaviglio P. (1985). La deformation cassante dans les calcaires Fuvéliens du basin de l'arc (Provence). PhD thesis. University of Provence, Marseille, France.

Pappas D.M., Mark C. (1993). Behaviour of simulated longwall gob material. Report of investigation no. 9458, US Department of the Interior, Bureau of Mines.

Al Heib (1993). Les nouvelles methods de modelisations numeriques et le volume d'influence des expolitations minieres en conditions complexes. Unpublished Ph.D thesis, Univ. Lorraine.